Performance Evaluation of Helical Separators Applied to Olive Oil–Water Two-Phase Flows at Low Reynolds Numbers

Pedro Vallesquino-Laguna [1,*], María Rivas-Valverde [1] and Inmaculada Pulido-Calvo [2]

1   Departamento de Bromatología y Tecnología de los Alimentos, Universidad de Córdoba, Campus Rabanales, N–IV, Km 396, 14014 Córdoba, Spain; mariarivas1987@hotmail.com
2   Departamento de Ciencias Agroforestales, Escuela Técnica Superior de Ingeniería, Campus El Carmen, Universidad de Huelva, 21007 Huelva, Spain; ipulido@uhu.es
*   Correspondence: bt1valap@uco.es

Abstract: One of the unit operations involved in the production of olive oil is the separation of liquid–liquid systems (and other multiphase flows) in their fundamental phases. The use of helical separators could be an alternative to be considered for that task in order to reduce energy consumption and improve the quality of products in olive oil mills ('almazaras'). In this work, four models of helical separators have been built and tested in order to manage olive oil and water two-phase flows (with olive oil as the majority phase). Separation yields were analyzed from a dimensional analysis perspective, considering variables such as density and viscosity, flow rate, head losses, or the water concentration in the flows studied. The best separation yields (of the order of 80% to 100%) were obtained for olive oil–water two-phase flows in which the water concentrations could be higher, in some cases, than 5–10% for Reynolds numbers of below 60.

Keywords: liquid–liquid system; dispersion; helical pipe; hydraulic system; separation yield

1. Introduction

Among the main objectives linked to food industry operations is the transformation or adaptation of incoming raw materials into manufactured products that meet the needs and wishes of consumers. Focusing our interest on a group of these industries, specifically those devoted to the production of olive oil (oil mills), one founds that it is a common problem to have to work with liquid–liquid systems (unstable suspensions or emulsions), liquid–solid or solid–liquid systems (suspensions and pastes) that have to be separated in their fundamental phases. In conventional practice, the aforementioned separations are usually carried out with techniques such as decantation (centrifugal or gravitational), sieving, or filtration, each of them having advantages and disadvantages with certain controversy [1–4]. In this sense, one could highlight that centrifugal decantation is usually considered as being a very fast, clean operation, but its energy cost can be high and the volume of wastewaters generated ('*alpechin*') can also be important. Gravity settling (using decantation tanks) is energetically less costly than centrifugation, but often provides slower separations, which can lead to sensory defects in the oil. With respect to sieving and filtration, it should be noted that these operations are complementary to the previous ones, as they are aimed at removing the small amounts of solids not retained in a previous decantation.

In this context, the use of helical separators (Figure 1), employed experimentally to treat water-oil systems associated with the petrochemical industry [5], could be an alternative to be considered in the olive oil mills area. It is worth noting that these devices do not require any moving parts, and they can easily be set up by using a cylinder shape in which a tube is coiled. Energetically they have fewer requirements than the centrifugal machines, and their residence (separation) times are low, of the order of seconds [6]. Regarding their internal dynamics (the behavior of the flow inside them), it can be pointed

out that the use of helical tubes has been extensively studied for one-phase flows under laminar regime [7–10] or under turbulent flow [11–13]. It is a characteristic of these types of streams that, together with the main movement of the longitudinal flow (along the axis of the pipe), two transverse vortices are present. These structures gradually lose their influence on the stream as the Reynolds number increases (as the flow transits from laminar to turbulent regime). Due to the action of the centrifugal force, the velocity profiles are not symmetrical in a given section, which signifies a further complication in understanding the behavior of this type of flows (see Figure 2 as an example).
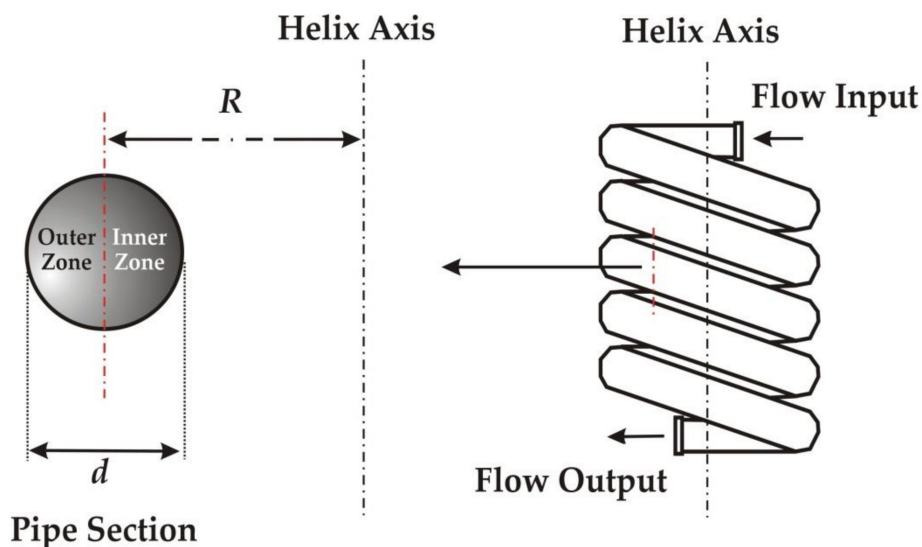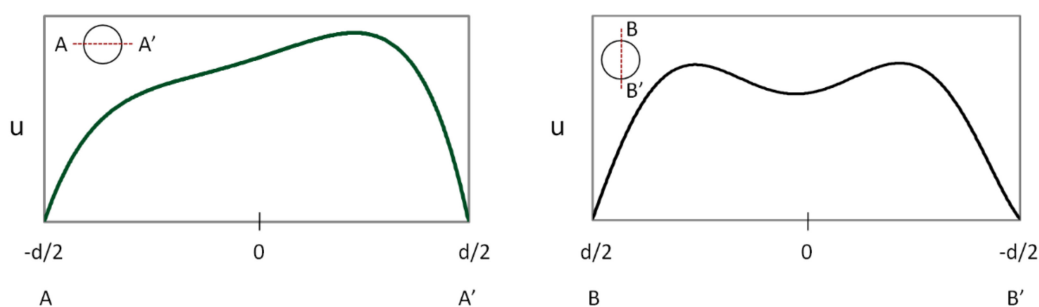

Figure 1. Scheme of a helical separator together with the detail of a section of the tube (*d* = pipe internal diameter; *R* = helix radius).

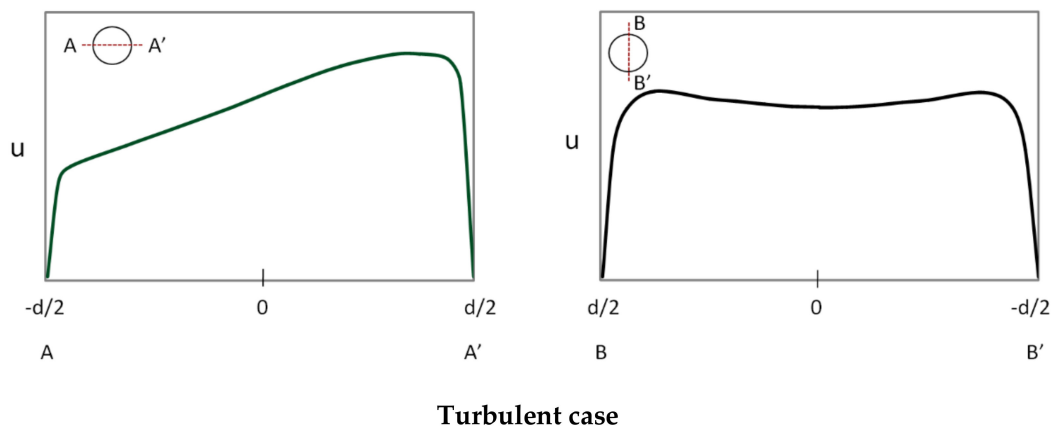**Laminar case**

Figure 2. *Cont.*

Turbulent case

Figure 2. Velocity profiles for helical one-phase flow under laminar regime (upper part) and turbulent regime (lower part) (*u* = flow velocity; *d* = pipe internal diameter).

In helical two-phase flows, a large part of research has been orientated towards those cases in which liquid–gas systems are analyzed [8,14–17], because the latter are frequently involved in industrial applications (such as power generation, refrigeration, heat recovery systems, etc.). Taking into account that liquids and gases show comparatively broad differences in their physical properties, it is reasonable to assume that the results of these studies may have limited value for other systems such as those formed by two liquids [18]. Studies made on water and oil two-phase flows in helical separators, are not numerous, which means that there is room for improving the design and operating conditions that could be of use for achieving acceptable separations with this type of technology. In this context, one reference work is that of Zhang et al. [19], in which, starting from tubes with an internal diameter *d* = 25 mm (with helix radius *R* = 150 mm or *R* = 400 mm), separation yields of close to 80% were obtained with water concentrations of around 40%. According to these authors, the separation efficiency of helical pipes depends on variables like: the helix radius, density difference between phases, residence time, pressure at the inlet and outlet or liquid droplet diameter. In this regard, for a given device, and thanks to the density difference between phases, when the flow rate is increased (by operating, for instance, the inlet pressure) or the helix radius is reduced, it is possible to obtain a higher centrifugal force. This usually leads to obtaining better separations if the turbulence disturbances are not too strong. This could be considered to be the key point of the performance of these devices: to achieve the highest centrifugal force with the lowest turbulence level. The above authors [19] also found that for low flow speeds, of the order (or less) of 1 m/s, the gravity force could have some influence on the distribution of water and oil within the duct, which allowed the obtainment of acceptable phase separations by making small discharge holes at the bottom of the helical tube outlet.

Other works like those of Zhao et al. [5,20] and Niu et al. [21] reported separation yields of close to 91% (for Reynolds numbers of the order of 7600) using a wide helix radius (*R* = 500 mm) with tubes of diameter *d* = 25.4 mm. In these studies, the maximum water concentration in the flow did not exceed 0.4%. From another viewpoint, by using pipes and helixes of a small diameter (*d* = 4 mm and *R* = 13.15 mm or *R* = 38.95 mm), Vallesquino and Molina [6] managed to obtain separation yields of close to 100% in water–oil two-phase flows, in which the oil concentrations were below 2% and the Reynolds numbers were less than 2000. With this in mind, and considering the usefulness and potential offered by this new alternative for the phase separation of liquid–liquid systems in any type of industry (especially in those devoted to olive oil production), this experimental work has aimed to study the behavior of these devices when they are applied to olive oil–water systems at different concentrations (water will be the minority phase). Separation yields will be analyzed, considering variables like the Reynolds number, head losses or water

concentrations in the flow, and some recommendations will be given that could be useful for future studies.

2. Materials and Methods

This section details the material and methods used in the experiments performed in this work. To this end, the elements that are part of the separators, and of the hydraulic system to which they were coupled, are presented. Then, the methodology applied throughout the experiments, in which these components were used, is described.

2.1. Separators

Taking into account the results and guidelines proposed by Vallesquino and Molina [6], together with the available resources, it was decided to build four helical separators using polyethylene pipe with a nominal diameter of 10 mm (inner diameter d = 9.45 mm plus 2 mm thickness). Two of these separators had a helix radius R = 34.05 mm, and the other two were constructed with R = 41.75 mm. In turn, for each value of R, two possible lengths (L) of tube were taken: L = 4 m and L = 7 m. In each separator, a length of 1 m was used for coupling the device to the hydraulic installation employed, leaving the rest of the tube (L—1 m) to construct the helical part of the device (Figure 3).
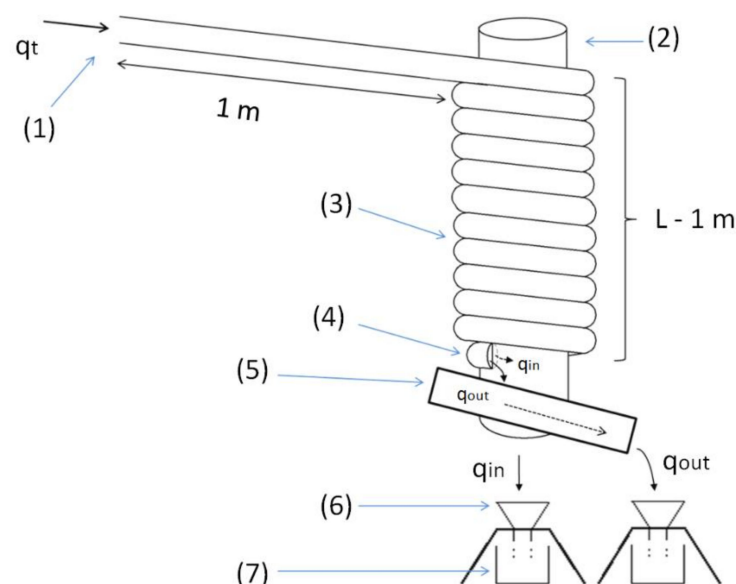

Figure 3. Helical separator scheme: (1) dispersion (emulsion) input; (2) coil mold; (3) helical pipe coil; (4) split zone; (5) gutter; (6) funnel; (7) vessel.

In each separator, the dispersion (or emulsion) to be treated was introduced under pressure from the top (see 1 in Figure 3), and at the lower end (4), at atmospheric pressure, the flow was split into two streams (q_{in} and q_{out}) by dividing the original pipe section into two equal semicircles, which were separated by the wall of the coil mold (that was 0.3 mm thick). The flows obtained were driven towards two separate funnels (6), and then into two different plastic vessels (7). With this approach, it was sought to disturb the streamlines at the end of the pipe as little as possible to prevent a water and oil remix.

2.2. Hydraulic System and Test Procedure

Figure 4 schematically depicts the hydraulic set-up used to test the separators cited above, in which the 19 mm PE pipe was generally used (except in elements (6) and (11)). In carrying out the experiments, a series of steps was followed with frequent repetitions. Next, the general procedure applied during the experiments is described taking as a reference the abovementioned Figure 4: firstly, and maintaining all the valves closed,

a 0.05 m^3 regulation tank (1) located at a level of about 7.5 m was filled with olive oil. Meanwhile, by gravity, the pipe stretch (1)–(2) was filled up with the oil from (1). After this, and through a removable coupling (5), water was supplied manually into the system by using a funnel that was momentarily coupled to a special stretch of 40 mm diameter pipe 1.5 m length (6). Subsequently, the rest of the system was filled up with olive oil by opening valves (3) and (3′). By means of a valve (4) it was possible to simultaneously purge the air that could be occluded in the ducts, thus eliminating any difficulty that might appear in this regard. This operation could be performed whenever necessary.
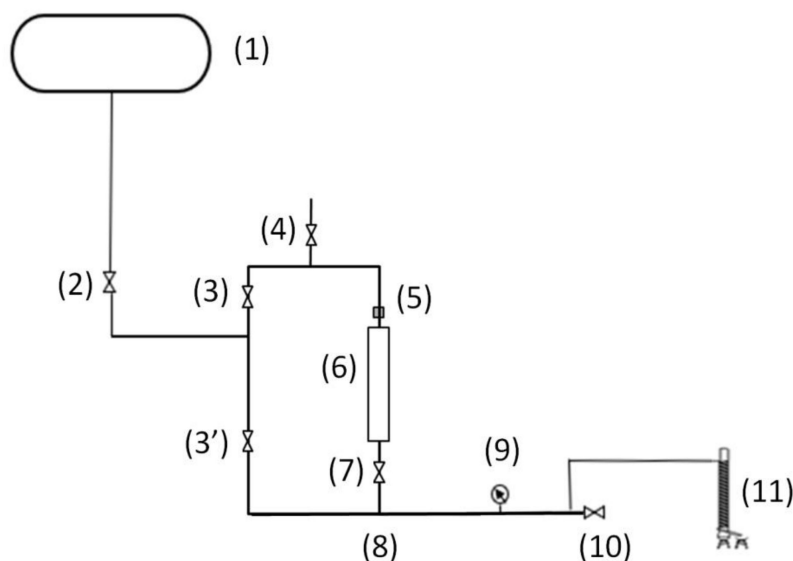

Figure 4. Hydraulic system scheme with: (1) olive oil tank; (2), (3), (3′), (7), and (10) auxiliary sphere valves; (4) air purge valve; (5) removable coupling; (6) water injector pipe; (8) oil–water mixing zone; (9) digital manometer; (11) helical separator.

Once olive oil and water have been fed into the hydraulic system by opening valves (3′) and (7), with a larger or smaller aperture, different concentrations of both fluids could be injected at the mixing zone (8). At point (9), a digital manometer was placed (with a maximum operating pressure of 20 m.W.C and accuracy of ±2%) to measure the pressure head at the inlet of the separator (11). In this context, numerous tests (not less than 20 per separator) were carried out at different pressure heads and outflow rates (as will be shown later) to analyze the hydraulic performance and separation yields of these devices under different conditions. In each experiment, the samples from the outer and inner sides of a given separator (Figure 5 as an example), were collected in coded and tared plastic vessels for their subsequent, efficient management. To enable the measurement of the volumes of olive oil and water contained in each sample, the following procedure was applied: samples taken in each experiment were stored and protected for further study. Then, they were weighed by using a laboratory scale with a precision of ±0.1 g. After this, the samples were placed in an oven at 105 °C for several days until the water was completely evaporated (checking the weights regularly until the final weight loss was verified). From the value of the last weighing, and the difference in the readings with respect to the pre-drying measurement taken, the weight of the oil and water content present in each sample could be estimated in each case. From this information, the corresponding volumes, of water and olive oil in each sample, could be computed by taking into account the density of each fluid. Accordingly, water density (ρ_w) was taken from the values tabulated in Singh and Heldman [22]; olive oil density (ρ_o) was estimated from the following experimental function [23], determined particularly for the olive oil used in these tests (in which *T* is

the oil temperature in °C, ρ_o is computed in kg/m^3, and S$_E$ = 2.040 kg/m^3 is the standard error):
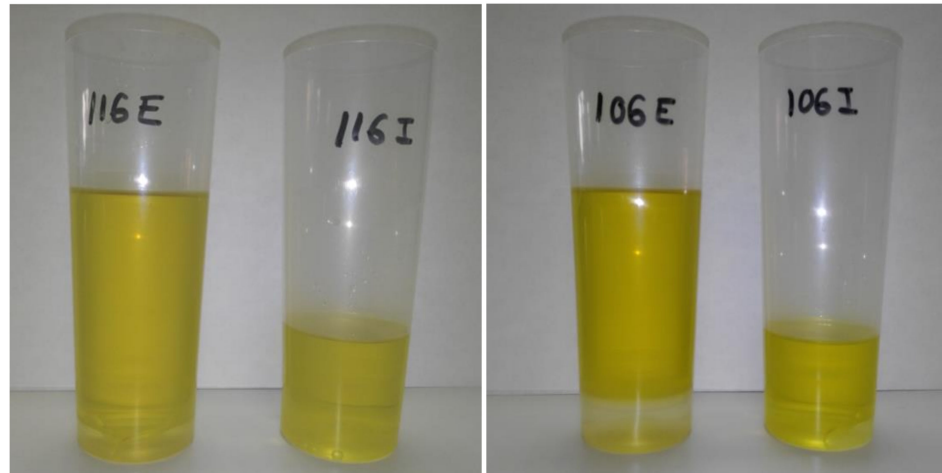
$$\rho_o = 932.262 - 0.977\,T \pm S_E \tag{1}$$

Figure 5. Outer (E) and inner (I) samples obtained in two experiments.

Once the volumes of olive oil and water were estimated in each sample, it was possible to determine the flow rates linked to them, since each sample was taken at a given time that was measured in each experiment using a digital chronometer (with an accuracy of ± 0.01 s). To ensure that all the experiments were conducted under similar conditions, the flow temperature was measured regularly in the tank (1), and at the separator outlets, with a digital thermometer (with an error of ± 1 °C). As all tests were performed under a stable environment, the flow temperature remained at around 25 °C in all cases.

3. Results and Discussion

Next, the results of the tests described in the previous section are presented and analyzed, on a theoretical basis assuming stationary flow, in order to ascertain whether helical separators are suitable for treating olive oil–water two-phase flows with adequate separation yields (η). Thus, it is reasonable to assume that, among very many other factors, physical properties such as fluid densities ρ_w and ρ_o, and dynamic fluid viscosities μ_w and μ_o, are variables that could be preliminarily taken to address the corresponding dimensional analysis of this problem. Note that subscripts "w" and "o" in each variable mean, respectively, that that variable is related to water or to olive oil. Beside the former, operating parameters like: the flow rate q, the pressure head h, temperature T, phase (water) concentration C (as a dimensionless fraction or percentage) and the inlet droplet diameter d_p (of the dispersed fluid) could also be integrated into this discussion. Moreover, geometrical variables like d (inner pipe diameter), R (helix radius), L (separator length) or Z (helix pitch) should not be forgotten. Finally, gravitational (g) or surface tension (γ) effects could also be accounted for, which could imply, overall, that the problem raised initially would signify managing 16 variables (including η).

As the previous approach could be difficult to handle, despite it being possible to reduce the number of variables by applying dimensional analysis methods, at this point, some assumptions need to be made to reduce the complexity of this question (leaving for future works those issues that could improve this study):

(1)   Since all the experiments have been developed under a stable flow temperature, variable T can be excluded in this case.

(2)   As the separators were built using the same helix pitch (Z was equal to the outer pipe diameter, see Figure 3), the effect of this variable on η cannot be evaluated, so this variable can also be excluded. Likewise, surface tension (γ) effects will not be

studied because the type (composition) of oil, water and pipe was not changed in the experiments, so that it becomes difficult to make any comparison.

(3)   The density and viscosity of the two-phase flows treated in the experiments can vary along each separator, because both parameters may depend on the water and oil concentrations, and on the type of mixture that may exist between them: homogeneous or heterogeneous, dispersion or emulsion, etc. So, as an approximation, the characteristic density and viscosity of a given flow (q) will be those linked to its majority phase (this issue will be discussed later). Considering this, ρ_w and μ_w will not be used in the dimensional analysis.

(4)   Given the material available in this study, there was no direct method for measuring the value of the inlet droplet diameter d_p. However, and due to the design of the hydraulic system used (see Figure 4), in practice it could be visually observed in the tests (for d_p sizes of the order of 1 mm, or even less), that the droplets of the dispersed fluid (water) depend on the ratio C/q (or equivalently, on C/h): the inlet droplet diameter tended to be small when q was high (elevated pressure in the system) and the water concentration C was reduced. Therefore, d_p could be indirectly accounted for, in this case, by the ratio C/q.

Applying the above, the following relation could be stated:

$$\Psi\ (\eta,\ \rho_o,\ \mu_o,\ q,\ h,\ C,\ d,\ R,\ L,\ g) = 0. \tag{2}$$

Knowing that the variables included in the previous equation are expressible in terms of the 3 basic units of mass, length and time, if the Vaschy–Buckingham π theorem principles are applied [24],

$$\eta\ =\ \varphi\left(\frac{d}{2R},\ \frac{L}{2R},\ \frac{4\,q\,\rho_o}{\pi\,d\,\mu_o},\ \frac{2gh}{\left(\frac{4q}{\pi d^2}\right)^2},\ C,\ \frac{\pi d^2 L \mu_o}{4\rho_o q R^2},\ \frac{\left(\frac{4q}{\pi d^2}\right)^2}{gd} \right) \tag{3}$$

can be obtained. According to the above expression, the separation yield η could depend on:

-   Geometrical relationships such as *d/(2R)* and *L/(2R)*.
-   On the Reynolds number:

$$Re\ =\ \frac{4q\rho_o}{\pi d\mu_o} \tag{4}$$

-   On the Euler number:

$$Eu\ =\ \frac{2gh}{\left[4q/(\pi d^2)\right]^2} \tag{5}$$

-   On the phase (water) concentration: *C*.
-   On the dimensionless factor $t_r{}^*$:

$$t_r^* = \frac{\pi d^2 L \mu_o}{4q\rho_o R^2}\ , \tag{6}$$

A version of the Fourier number [24,25], adapted to a stationary momentum transfer context, that is related to the residence time t_r:

$$t_r\ =\ \frac{\pi d^2 L}{4q} \tag{7}$$

- And finally, on the Froude number:

$$Fr = \frac{\left[4q/\left(\pi d^2\right)\right]^2}{gd} \tag{8}$$

In view of the above, and taking into account the experimental design presented in Section 2, the results of the tests carried out will be analyzed by comparing the performance of the available separators (four different geometries), when the Reynolds, Euler and Froude numbers, as well as C and $t_r{}^*$, are considered. Moreover, some other relationships, that could help to understand the behavior of these devices, will also be studied.

3.1. Reynolds Number vs. Total Flow Rate

As the flows treated in this study are composed of two phases (olive oil and water), it is not easy to estimate with any accuracy the actual Reynolds number which may exist in any flow section (or stretch), since the density and viscosity of these flows can be variable along the duct. In order to solve this problem, one can roughly assume that, through an apparent value of the Reynolds number, the information available can be analyzed to extract useful considerations [6]. That apparent Reynolds number (Re_a) can be estimated by means of Equation (4), also assuming that $q = q_o$ (the flow is characterized by the values related to its majority phase, in this case olive oil):

$$Re_a = \frac{4 q_o \rho_o}{\pi\, d\, \mu_o} = \frac{4\, q_o}{\pi\, d\, v_o} = \frac{U_o\, d}{v_o} \tag{9}$$

where the subscript "o" in each variable, remember, is related to olive oil, and v and U are, respectively, the kinematic viscosity and the average flow velocity. In this work, the value of ρ_o (in kg/m^3) was determined by applying Equation (1) (see Section 2.2) and the value of μ_o (in Pa·s) was estimated from an experimental function [23], that was obtained for the olive oil used in these tests, and in which T represents the oil temperature (expressed in °C) and $S_E = 0.002$ Pa·s is the standard error:

$$\mu_o = -0.0037\, T + 0.177 \pm S_E \tag{10}$$

Obviously, the value of the olive oil kinematic viscosity (v_o) can be deduced from ρ_o and μ_o considering that $v_o = \mu_o/\rho_o$. In addition, the formulation of Equation (9) has been established taking into account the relationship that can be formulated between the average flow velocity (U) and the flow rate (q) for any incompressible fluid:

$$U = \frac{q}{A} = \frac{q}{\pi\, \frac{d^2}{4}}, \tag{11}$$

in which A is the area of the pipe section. According to Equations (9) and (11), the value of U_o must also be taken as an apparent value, since it has been estimated from a flow rate (q_o) that does not fully fill the pipe section through which it flows (please note that water is also present in the two-phase flow). In the scientific literature, any U value calculated in this way is usually known as superficial velocity [6,26]. Besides the Reynolds number, in this manuscript section the total flow (q_t), which circulates through each separator in any experiment, has been considered to be a variable of interest because it serves to indicate the processing capacity of the separators built (on scale). This flow can be calculated as being the sum of the olive oil flow (q_o) plus the water flow (q_w) which are present in each test ($q_t = q_o + q_w$). From another perspective, the flow q_t can also be equally estimated as: $q_t = q_{in} + q_{out}$. In this case, q_{in} and q_{out} are, respectively, the flow rates collected from the inner and the outer sides at the end of the separator (see Figure 3). In Figure 6 the values of total flow q_t (in l/h) are shown as a function of the apparent Reynolds number Re_a for the four different geometries used (remember that their characteristics are detailed in Section 2.1).
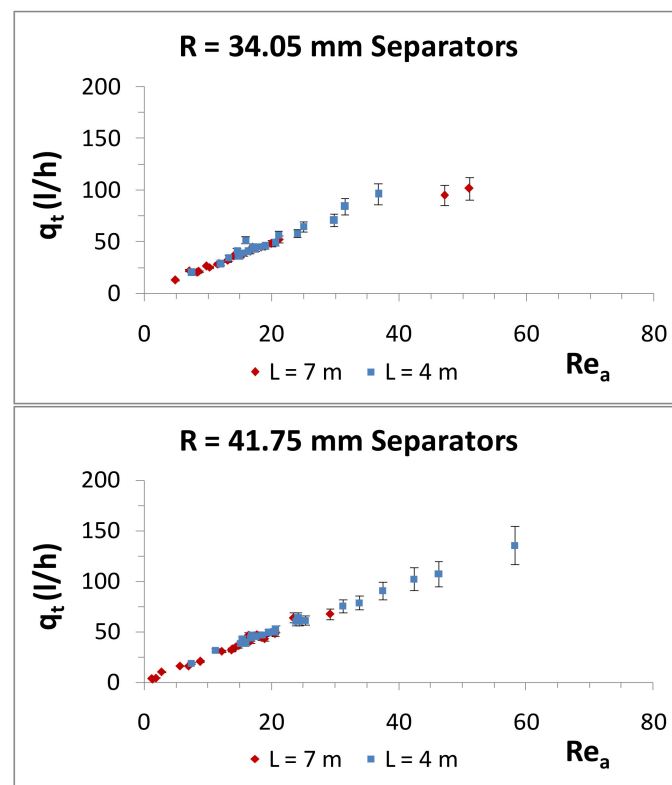
Figure 6. Relationship between the apparent Reynolds number Re_a and the total flow q_t (l/h) for the separators tested with different helix radiuses R (34.05 mm and 41.75 mm) and tube lengths L (4 and 7 m).

In general, from the results obtained, it is worth highlighting that the four separators follow a similar behavior, clearly observing how, as the apparent Reynolds number increases, the total flow rate (less than 140 l/h in all cases) augments almost linearly. Given the viscosity of the majority phase (see Equation (10)), Re_a values in all tests have been very low (within a range from 0 to 60). This fact allows one to assume in advance—in the absence of other results that will be shown later—that the experiments have been conducted under laminar flow if the criteria established by Srinivasan et al. [27], for single-phase flows, is roughly accepted:

$$Re_{crit} \approx 2100 \left(1 + 12\sqrt{\delta}\right) \tag{12}$$

where Re_{crit} is the critical Reynolds number in which transition starts and $\delta = r/R$ is a factor given by the ratio between the pipe radius (r) and the helix radius (R). In this study, Re_{crit} could be of the order of 10,000 in all separators, a much higher value than $Re_a = 60$. At this point, what deserves a mention is that, despite the experiments presented in this research having been run on scale, they could be of use for other works, because in food processing it is very usual to handle low Reynolds numbers (as food fluids usually have large viscosities). As an example, for an olive oil production of 3000 l/h –a common flow rate treated by the centrifugal separators in the 'almazaras'– [6,28] Re_a could, in many cases, be of the order of 200. This Re_a value is not very far from those presented in Figure 6. With a different approach, Zhao et al. [5,20] or Niu et al. [21] proposed using helical separators for values of Re_a just above Re_{crit}, but, as will be discussed later, this solution may not be the most suitable one for reaching good separation yields for water concentrations like those addressed here. In this respect, and using water as a majority phase, Vallesquino and Molina [6] observed that for $Re_a > 2000$ it was not possible to achieve good separations, regardless of the oil concentration values, due to the agitation (turbulence) present in the flow.

3.2. Reynolds Number vs. Pressure Head and Euler Number

In the dimensional analysis made above, a generic pressure head term (h) was included as one of the operating parameters that could have some influence on the separation yield η. This term could be represented by the pressured head at the inlet (or the outlet) of the separator, or by the pressure head difference between both ends. As the discharge of these devices was at an atmospheric pressure, the following could be accepted:

$$h = h_{fk} \approx H_i + \Delta z \tag{13}$$

in which h_{fk} are the head losses occurring along the separator, H_i is the pressure head at its inlet and Δz is the difference in height between the inlet and outlet points. As an approximation, velocity heads have been neglected because they are small and are mutually offset between the separator ends. According to this, Figure 7 displays the values of head losses h_{fk} in each separator, as a function of Re_a, to establish (on scale) the energy requirements of these devices. Results displayed in that figure show a roughly linear trend in all the separators, which indicates a direct (practically proportional) relationship between the energy losses and the Reynolds number Re_a (which will be used to understand other results analyzed later). Moreover, some scattering is observed in the values shown in Figure 7, which could be explained by the difference in water concentrations in the tests, and by the mixing degree in the olive oil and water. As is usual in this context, the results of h_{fk} can also be expressed as a function of a friction factor. If the Euler number included in Equation (3) is multiplied by the geometric factor d/L (a linear combination of terms $d/(2R)$ and $L/(2R)$ from Equation (3)), the following could be deduced, taking into consideration the Darcy–Weisbach equation [24]:

$$f_a = \frac{2gh_{fk}}{(4q_o/(\pi d^2))2} \frac{d}{L} = \frac{2gh_{fk}}{U_o^2} \frac{d}{L} = Eu_a \frac{d}{L}, \tag{14}$$

in which f_a has to be taken as an apparent friction factor because it is based on the olive oil flow q_o (that also implies that the Euler number is computed through an apparent value Eu_a). It should be noted that Equation (14) has been formulated under the hypothesis that h_{fk} has the same value (from Equation (13)) for q_o and q_t (as the pressure head for both flows was the same at the inlet or at the outlet of each separator).
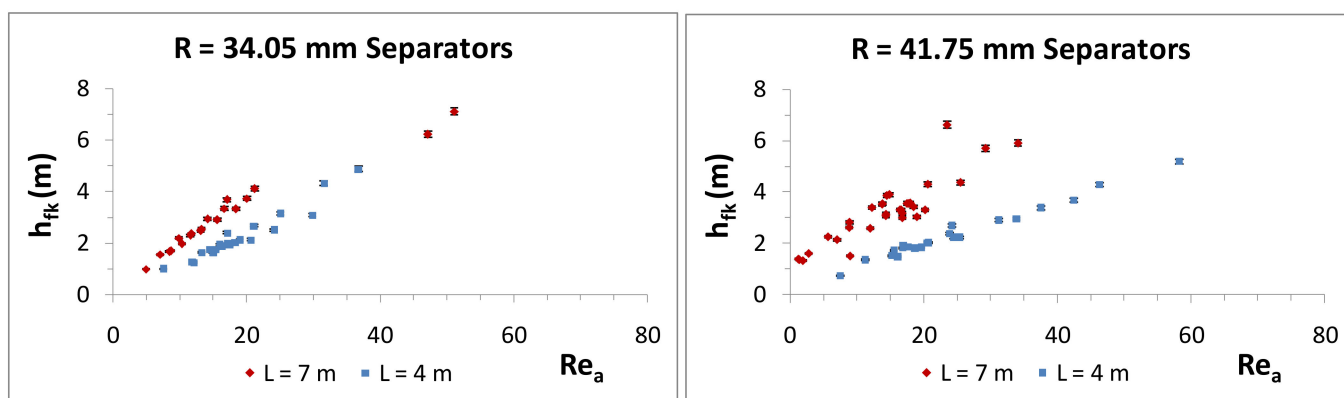

Figure 7. Relationship between the apparent Reynolds number Re_a and the head losses h_{fk} (m) for the separators tested with different helix radiuses R (34.05 mm and 41.75 mm) and tube lengths L (4 and 7 m).

On the basis of the above, Figure 8 shows the experimental values of f_a (obtained from Equation (14)) together with a rough estimation of this factor (f_{aI}) that can be made from an adaptation of the Ito equation, that is valid for helical single-phase laminar flows [13]:

$$f_{aI} = \frac{64}{Re_a} \frac{21.5\,De_a}{(1.56 + log_{10}De_a)^{5.73}},$$

(15)

where De_a is the apparent Dean number that can be calculated from Re_a:
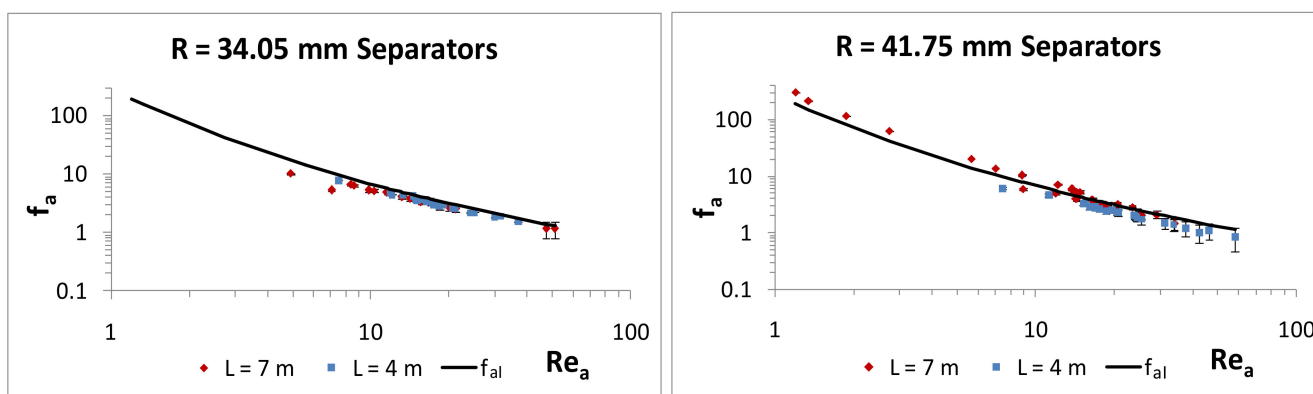
$$De_a = Re_a\,[d/(2R)]^{0.5}$$

(16)

Figure 8. Relationship between the apparent Reynolds number Re_a and the friction factors f_{aI} and f_a for the separators tested with different helix radiuses R (34.05 mm and 41.75 mm) and tube lengths L (4 and 7 m).

In analyzing Figure 8, worth a mention is the approximation that exists between the theoretical and the experimental data of the friction factor f_a, despite the Ito equation being originally established for helical single-phase flows. This fact reinforces the idea that the flow regime in the experiments was predominantly laminar and it was dominated by the main phase, which also had a higher viscosity than the minority phase. This circumstance confirms what was already commented on in the previous section in relation to the low Re_a values recorded and the performance of q_t. In this sense, it could be verified that between the head losses h_{fk} and the flow rate q_t there is also an increasing linear relationship (with some degree of scattering), that is compatible with the existence of the laminar flow.

The preceding results could be of interest for future works in this field, since in the literature of helical separators [5,6,19–21] the Darcy–Weisbach friction factor is usually not calculated or analyzed. In helical two-phase flows, focused on gas–liquid systems [8], deviations have been reported of the order of, or less than, 30% (between single-phase and two-phase flow friction factors) for volumetric water concentrations of below 0.3%. These deviations are of the same order of the ones addressed here, but in this study the water concentrations applied were higher (as presented next in Sections 3.3 and 3.5).

3.3. Reynolds Number vs. Water Concentration, t_r^* and Froude Number

Figure 9 displays the values of water concentration C (as a percentage) as a function of the Reynolds number (Re_a) in each experiment. The values of C are obtained from the ratio between the water flow rate q_w and the total flow rate q_t: $C\,(\%) = 100 \cdot q_w / q_t$. It is noteworthy that these flow rates can be obtained by simple arithmetic from the samples taken, in a given time and in each test, once the volumes of oil and water have been determined according to the procedure already described in Section 2.2.
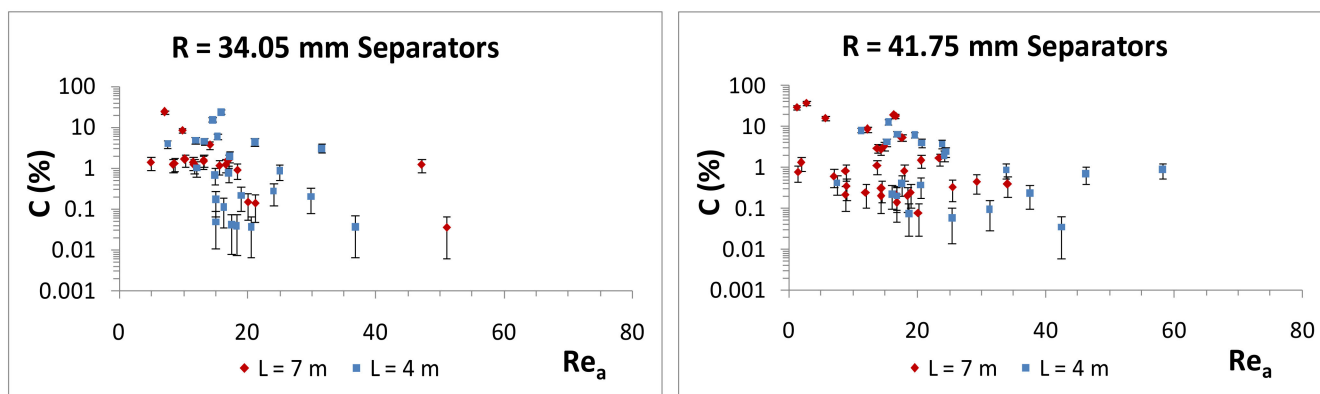
Figure 9. Relationship between the apparent Reynolds number Re_a and the water concentration C (%) for the separators tested with different helix radiuses R (34.05 mm and 41.75 mm) and tube lengths L (4 and 7 m).

In observing Figure 9, it is notable that, in general, C is less than 10% in most of the experiments, but there are some cases in which this variable can reach values of the order of 30–40%. Comparatively, reference could be made to the work of Vallesquino and Molina [6], which described water–olive oil systems with olive oil concentrations of less than 12% (water was the majority phase with $C > 88$%). In other studies [5,20,21], related to water–mineral oil systems, this problem has been mainly tackled from a theoreticalsimulation perspective by presenting some laboratory experiment results mainly linked to an oil concentration of 0.4% ($C \approx 99.6$%). Other authors [19], with a similar approach, presented the results of four tests, in which water concentrations seem to vary from 39.8–64.4%. In view of the above, it is reasonable to assume that, in the field of the food industry (and especially in applications related to edible oils), the present study could be of use for future works interested on helical separator technology.

Regarding the distribution of C in Figure 9, it should be noted that this factor seems to vary in each separator in an apparently erratic way, with no relationship with the Re_a values. Since the injection of the water into the system was not carried out by following an established flow or pressure pattern, it is normal for no relationship to be observed between these variables. However, as was stated at the beginning of Section 3, since the droplets of the dispersed fluid (water) depend on the ratio C/q, that zone in Figure 9, where Re_a is high and C is small, could probably be related to small droplet size experiments (note that q_t is proportional to Re_a according to Figure 6). On the contrary, where C is high and Re_a is small, the droplet size expected could probably be larger. Considering this, Figure 9 shows that the tests could have been run with a great variety of droplet sizes.

On the other hand, if Figures 7 and 9 are observed together, a certain relationship seems to be established between the variability of C and the scattering of h_{fk}. In this sense, the data from the separator with $R = 41.75$ mm—$L = 7$ m, and from the case with $R = 41.75$ mm—$L = 4$ m, are worth highlighting, because the former has the most dispersed values of C and h_{fk}, and the latter shows the least dispersed values of those variables. Viewing this, it is reasonable to suppose that the more the C values differ in the tests, the more the variability in the viscosity present in the flows, which will result in a wider scattering of h_{fk}. Likewise, the degree of mixing (or emulsification) in the flow can also influence this variability, a fact that could explain the scattering that h_{fk} shows, for $Re_a > 20$ and C < 2%, in the separator with $R = 41.75$ mm—L = 7 m (a great dispersion of h_{fk} is observed in Figure 7, despite the fact that C changes very little in Figure 9 for the referred range of Re_a).

As for the relationship between the Reynolds number and t_r^* (Equation (6)), it should be noted that this dimensionless variable depends on $q = q_t$ (or in $q = q_o$ if it is decided to compute the apparent value $t_r^*_a$) and on some other factors that, for a given separator and fluid (olive oil), are constant. In this situation, and as $q_t = f(Re_a)$ (see Figure 6), it follows that t_r^* is a simple function that depends on $1/Re_a$, and no extensive analysis is required, because no relevant results would be obtained. A similar approach can be made with the

Froude number *Fr* (Equation (8)), which ultimately could be expressed, in this case, as a simple function of $(Re_a)^2$.

3.4. Reynolds Number vs. Separation Yield

Once the different terms included in the second member of Equation (3) have been studied, it is time to take into consideration the separation yield (η) and its relationship with these terms. In this respect, it is necessary to establish the following expression to determine the relative separation yield (η) associated with a given test:

$$\eta = \frac{q_{w_{out}}}{q_w}\,100 = \frac{q_{w_{out}}}{q_{w_{in}} + q_{w_{out}}}\,100, \tag{17}$$

where q_{wout} is the water flow rate collected from the outer side of the separator and q_w, according to Section 3.1, is the water flow rate entering the separator ($q_w = q_{win} + q_{wout}$, with q_{win} as the water flow rate from the inner side of the separator). As an example, Figure 10 shows an image of one of the tests performed, in which the main part of the water flow rate is present on the outer side of the separator, and the oil flow rate is basically placed on the inner side. As expressed in Equation (17), a relative separation yield is equal to 100% when $q_{wout} = q_w$ (the water is collected in its totality from the outer side and $q_{win} = 0$). If $q_{wout} = 0$ it so happens that $q_w = q_{win}$, and the separation yield η will be null, which implies that the water is completely extracted from the inner side of the separator (an undesired situation because the water would be expected to be collected from the outer side as it is a denser fluid than oil). These two cases are extreme, but they help to interpret the results that are presented below. To this end, Figure 11 shows the values of η as a function of Re_a for the separators tested. On the whole, from the cited figure it is highlightable that, from a given Re_a value, the separation yields improve, reaching values of between 80% and 100% in most cases. Specifically, for approximately $Re_a > 15$, acceptable η values can be observed in all the separators, so that it can be inferred that these devices comply with the purpose for which they were designed. On these lines, also notable is the performance of the separator with $R = 41.75$ mm—$L = 4$ m, which presents values of above 80% in practically all the experiments (even for $Re_a < 15$). However, the fact that for $Re_a > 15$ there may be other cases in which $\eta < 80\%$ suggests that Re_a is not the only variable to take into account for establishing the best operating conditions. That is why, in the next sections, more relationships between parameters will be explored to verify which variables could be the most significant ones to consider.
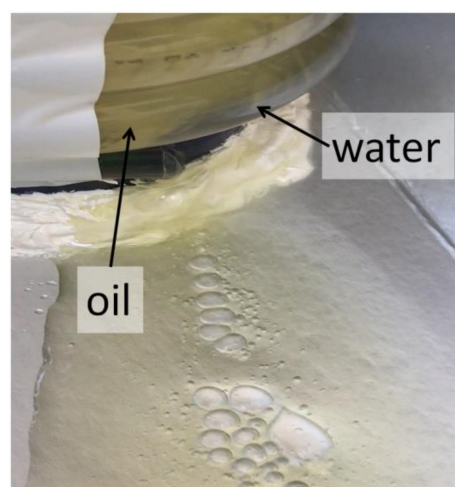

Figure 10. Example of test made: the main part of the water flow rate is present on the outer side of the separator and the oil flow rate is basically placed on the inner side.
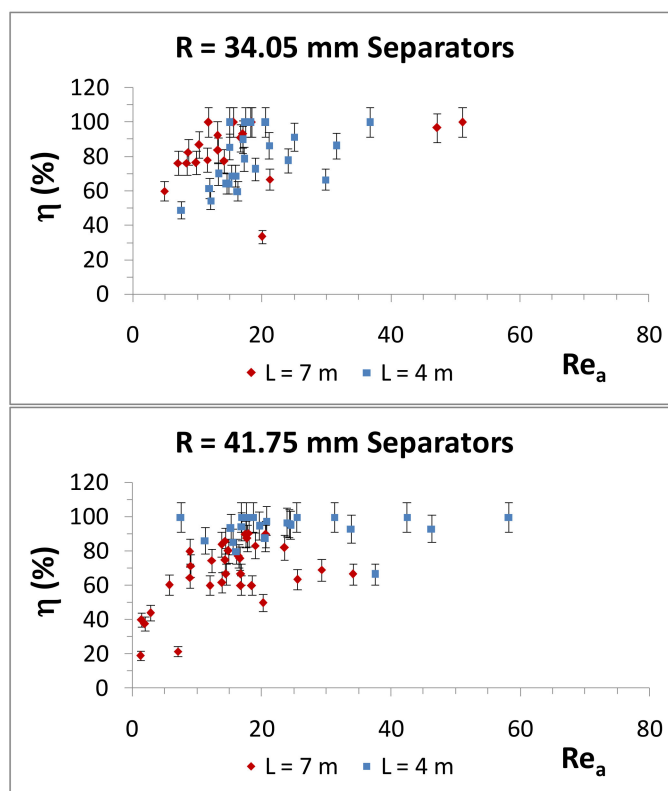
Figure 11. Relationship between the apparent Reynolds number Re_a and the relative separation yield η (%) for the separators tested with different helix radiuses R (34.05 mm and 41.75 mm) and tube lengths L (4 and 7 m).

Apart from the above, and directly related to the contents of Section 3.1, it is also notable, see Figure 11, that, to achieve an acceptable separation yield, it is not necessary to reach high Reynolds numbers. On the contrary, and according to Vallesquino and Molina [6], it is desirable to work under $Re_a < 2000$, a value that is usually much lower than Re_{crit} (see Equation (12)). In this context, Zhang et al. [19] discuss a case in which the separation yield was of the order of 80% for a flow rate that could be linked to $Re_a \approx 300$ (if the criterion established in Equation (9) is accepted). Other studies [5,20,21] proposed working with flow rates that, accepting Equation (9) used here, would be associated with $Re_a \approx 7600$. That value (just above Re_{crit} in those studies) could, in many cases, not be conducive to achieving good separation yields [6], which adds some controversy to this field and justifies the need for more research.

3.5. Water Concentration vs. Separation Yield

Similarly to the above section, the separation yields η are represented in Figure 12 as a function of water concentrations C (%), taking into account that C does not exceed 40% in any of the cases.
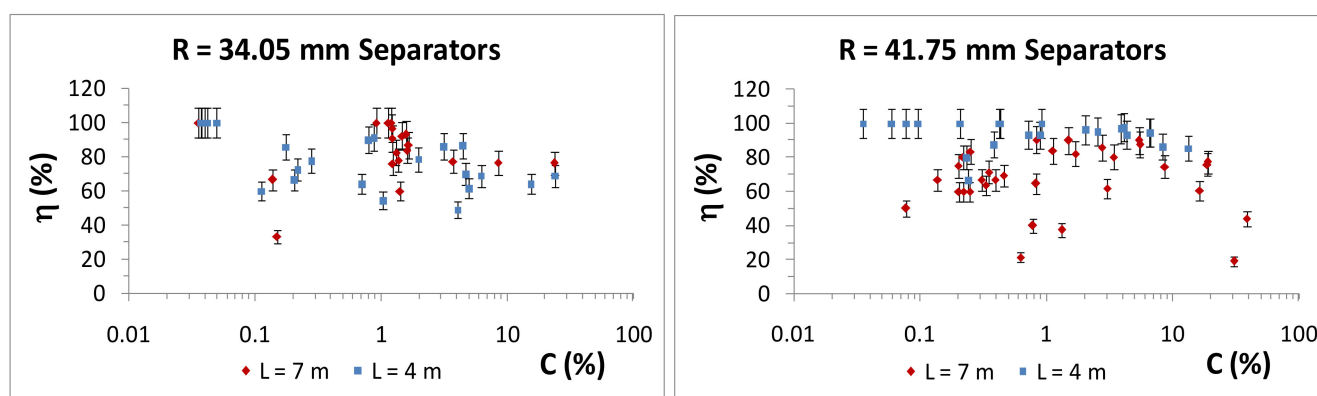
Figure 12. Relationship between the water concentration C (%) and the separation yield η (%) for the separators tested with different helix radiuses R (34.05 mm and 41.75 mm) and tube lengths L (4 and 7 m).

It can be seen that, at very low water concentrations, the variability of separation yields η is high, which suggests that the water concentration C, by itself, is not the only variable to be considered in the search for adequate separations. However, the best performance values ($\eta > 80\%$) seem to generally be linked to a working area in which $C < 5\%$. From this value ($C > 5\%$), there seems to be some stability of η, tending to be in the range of 60–80%. This working area is not deficient, but it could be improved, which sets a context in which advancement in the design or handling of these devices could be studied. For its part, the separator with $R = 41.75$ mm and $L = 4$ m seems to maintain good results ($\eta > 80\%$) even for $C > 5$–10%, which underscores this idea. As was remarked in Section 3.3, there are few studies addressing the relationship between phase concentrations and separation yields in helical devices. According to Vallesquino and Molina [6], it is not recommended to work with oil concentrations of above 2% in water–olive oil systems. In other studies [5,20,21], in the field of water–mineral oil systems, very acceptable separation yields could be obtained for oil concentrations of the order of 0.4%. Other authors [19], report one case (in mineral oil–water systems) in which, for a water concentration of close to 47%, it was possible to reach a separation yield of the order of 80%. Analyzing these references and the data presented herein, it seems reasonable to consider that η, in oil–water systems, could be greater at higher concentrations of the minority phase (C_{mp}) than in water–oil systems, which could be due to the viscosity of the majority phase. As any oil is usually more viscous than water, the flow tends to be more stable in oil–water systems (there is less turbulence) than in water–oil systems for a given C_{mp} value. This agrees with the assumption that the separation phenomena are normally promoted in those systems less affected by disturbances [28].

3.6. Ratio Re_a/C vs. Separation Yield

From Sections 3.4 and 3.5 it is deduced that there are two conditions for obtaining the best separation yields. On one hand, it has been verified that, from a certain value of Re_a (variable directly linked to the energy available for the separation), the η yields reached could be considered as being acceptable. Regarding water concentration, it would seem that the separation yields are not adequate for large C values, but this condition does not imply that for small C values η could be appropriate. This section has studied how the ratio Re_a/C can have an influence on the yield η. To this effect, if the considerations expounded at the beginning of Section 3 are respected, as well as the relationship between q_t and Re_a (see Figure 6), it follows that the factor Re_a/C is directly related to the inlet droplet diameter of the dispersed fluid (visually it was observed how, as Re_a/C was increased, d_p tended to decrease under values that could be of the order of 1 mm or even less). On the other hand, it should be noted that Re_a/C is also linked to the energy level available in each experiment (as h_{fk} is proportional to Re_a because the flow is predominantly laminar, see Figures 7 and 8).

For those reasons, in Figure 13 the values of η are displayed as a function of those of Re_a/C (taking C as a percentage) from certain threshold values that seem to be characteristic in each separator. Considering these results, it is reasonable to assert that, with enough energy and adequate water concentrations (Re_a/C higher than 5–10), the separators constructed can provide adequate separation yields. Since Re_a values have been limited in this work (given the means available), the separation yields (in general) have not been satisfactory for water concentrations $C > 5\%$. However, according to the results presented in Figure 13, it seems possible to guess the likelihood of obtaining better separation yields, for water concentrations $C > 5\%$, if the energy available were to be greater (maintaining $Re_a/C > 5$–10). This opens up an area for improvement that should be considered in future works. The fact that C has to be higher than a certain threshold value (of the order of 0.4–0.9% depending on each separator) might be explained by the mixing or emulsion degree reached by the flow. In this respect, it must be noted that after re-using the same olive oil on successive occasions with the same separator, part of it was intimately emulsified with the water used (in these cases, d_p could probably be of the order of some microns), and that phase was hardly separable. Hence, below a certain water concentration C (not controllable) the separation yields were not as expected and the head losses h_{fk} were randomly scattered in some tests (remember the information in Section 3.3).
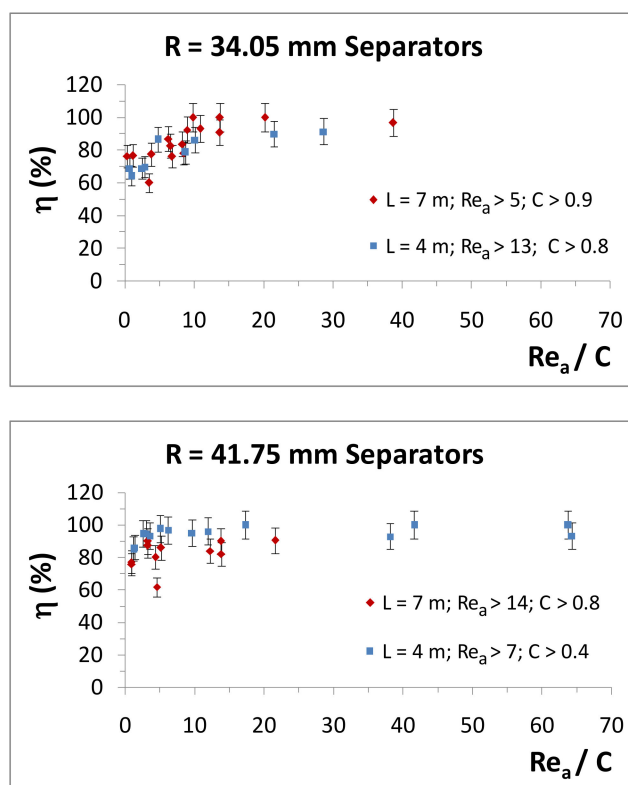

Figure 13. Relationship between ratio Re_a/C and η (%) for the separators tested with different helix radiuses R (34.05 mm and 41.75 mm) and tube lengths L (4 and 7 m).

In the works directly related to this study [5,6,19–21], the influence of Re_a/C on η has not been properly studied. Despite this, it could be argued that, in water–olive oil systems [6], the best separations yields were obtained for $500 < Re_a/C < 22,000$ (with $Re_a < 2000$, $C < 2\%$). In the works of Zhao et al. [5,20] and Niu et al. [21], the experimental results analyzed show that for $Re_a/C \approx 19,000$ (with $Re_a \approx 7600$) it was possible to obtain good separation yields in water–oil systems. In the study of Zhang et al. [19] on oil–water systems, the best separation yield was found for $Re_a/C \approx 6.6$ and $Re_a \approx 300$. On the whole, the values of Re_a/C presented here are in the smaller range of those in which acceptable

separation yields have been reported. This again makes it possible to expect (as was indicated above) that in olive oil–water systems the ratio Re_a/C could be higher to reach adequate η values for water concentrations C > 5%.

3.7. Separation Yield and Other Terms

In order to gain a better understanding of the minimum energy level required to achieve adequate separations in the models built, the head losses h_{fk} and the separation yields η have now been analyzed comparatively. The relationship between these variables is shown in Figure 14, in which it stands out that, from a certain level of h_{fk} (of the order of 2–3 m depending on each device), the separation yields can be quite appropriate, even next to 100%. However, for this energy level there are also low η values, which could be explained by an inappropriate water concentration (too high to reach a ratio $Re_a/C > 10$, see previous Section 3.6). Additionally, it has been seen that, when h_{fk} is below 2–3 m, the separation yields generally begin to worsen. Again, it has been observed that when the available energy is low, the separations are often not good ones, because there is a lack of centrifugal force in the flow.
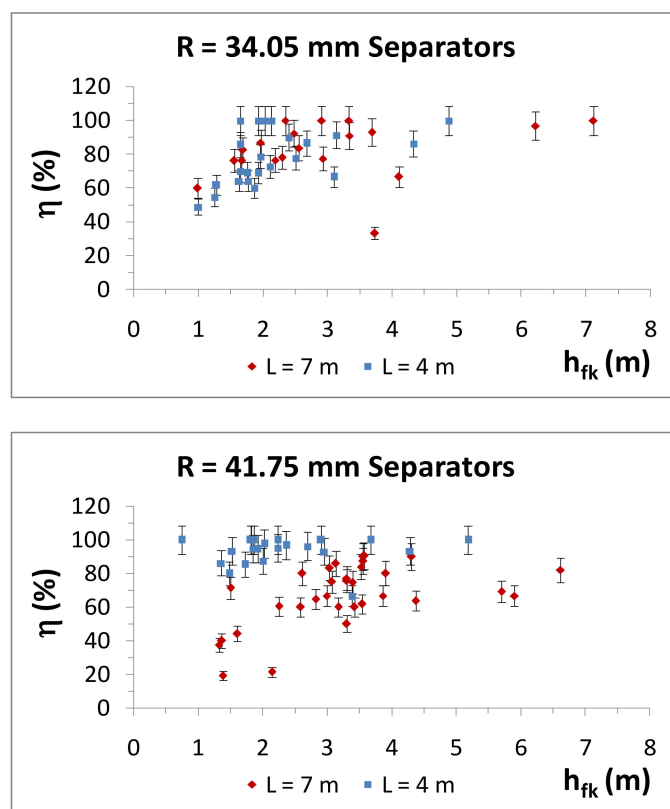

Figure 14. Relationship between h_{fk} (m) and η (%) for the separators tested with different helix radiuses R (34.05 mm and 41.75 mm) and tube lengths L (4 and 7 m).

With regard to the relationship between the Euler number (*Eu*) and the separation yield (η), this is shown in Figure 15, taking as a reference the definition of the apparent value Eu_a just defined in Equation (14). In general, the conclusions that can be extracted from this figure are similar to those obtained from Figure 11, in which Re_a and η were addressed. Again, the performance of the separator with $R = 41.75$ mm—$L = 4$ m is striking, and, for a certain range, the studied devices offer acceptable separation yields (though in that zone there are also points with bad separations). The only difference to be pointed out is that the data distribution in the relationships between Re_a and η, and between Eu_a and η (Figures 11 and 15), follow opposing linear trends. The explanation to this can be

supported by the relationship that can be established between Re_a and $Eu_a = f_a \cdot L/d$ (see Equation (14) and Figure 8). Since f_a (or Eu_a) is inversely proportional to Re_a, the trends that could be present in these figures should be inverse of each other.
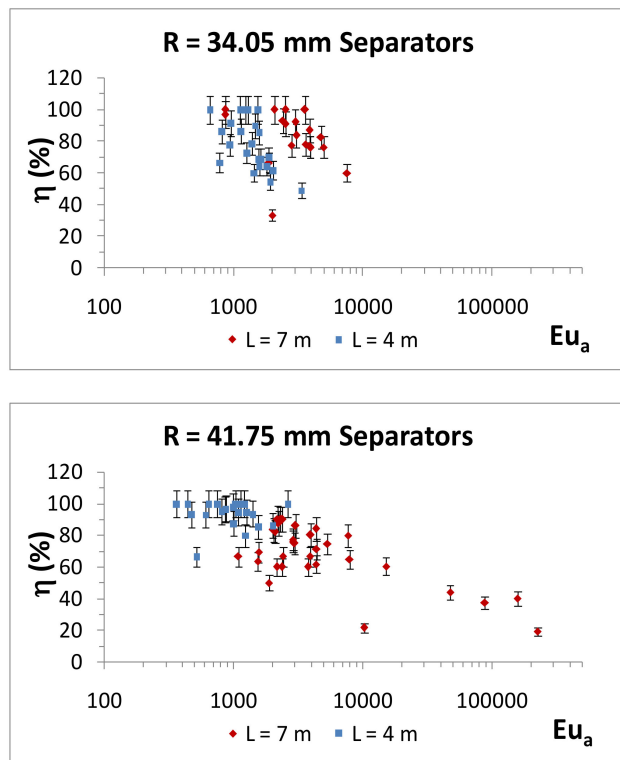

Figure 15. Relationship between apparent Euler number Eu_a and η (%) for the separators tested with different helix radiuses R (34.05 mm and 41.75 mm) and tube lengths L (4 and 7 m).

By the same logic, Figures 16 and 17 display the results of η as a function of the dimensionless time t_r^* (Equation (6)) and the Froude number Fr (Equation (8)) considering, in both cases, that $q = q_t$. It is characteristic in these figures for the distributions of the points represented to be very similar to those given in Figures 11 and 15, respectively, since $t_r^* = f(1/Re_a)$ and $Fr = f(Re_a^2)$, as was stated in Section 3.3. This fact allows one to surmise (in this particular case) that the possible influence of t_r^* or Fr, on the yield η, can be accounted for through Re_a, which could help simplify the analysis of this question in cases similar to the ones dealt with in this study.
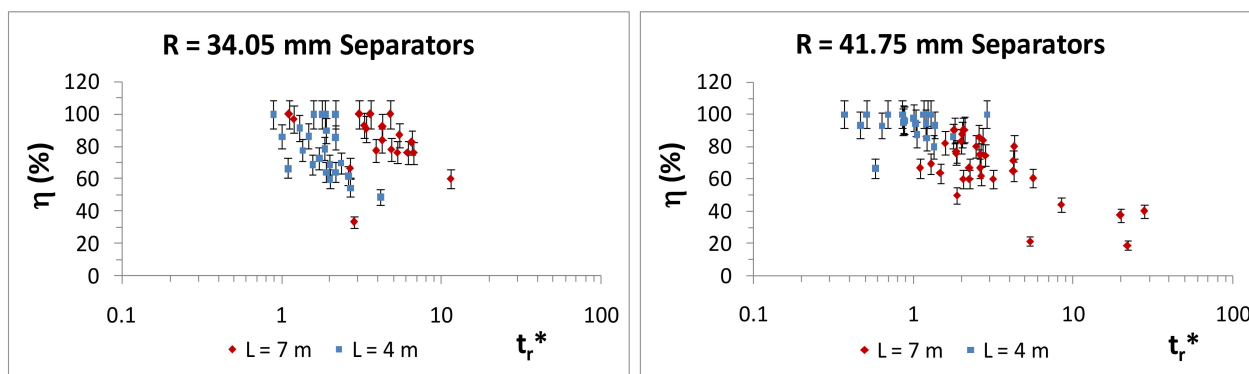

Figure 16. Relationship between t_r^* and η (%) for the separators tested with different helix radiuses R (34.05 mm and 41.75 mm) and tube lengths L (4 and 7 m).
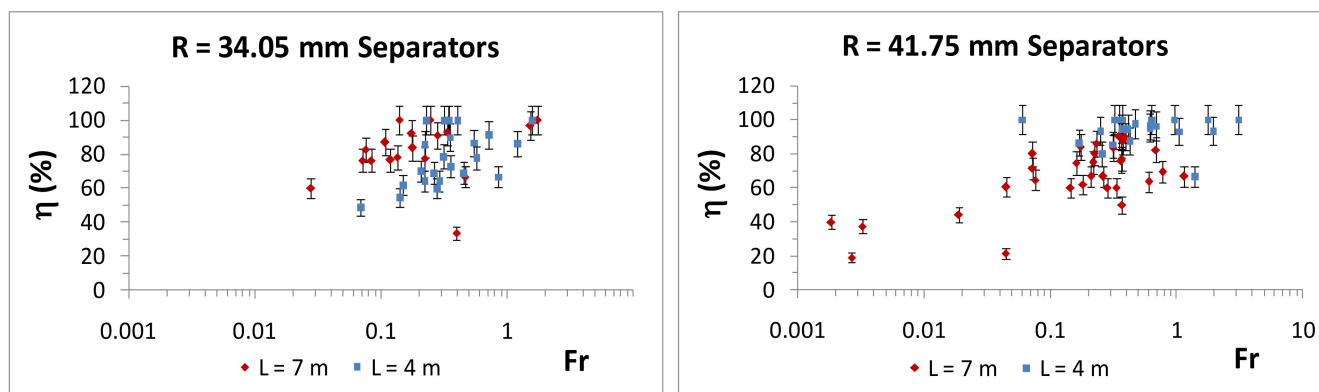
Figure 17. Relationship between Froude number *Fr* and η (%) for the separators tested with different helix radiuses *R* (34.05 mm and 41.75 mm) and tube lengths *L* (4 and 7 m).

As an example of the above, and taking into account the designs shown in Figures 1 and 3, it is obvious that, in order to achieve an adequate separation yield, the water flow in any test should be placed at the outer zone of the pipe section (not at the bottom part of the duct). This situation can only be reached if the centrifugal force is more important than the gravitational one, which implies that the Reynolds number (or the Froude number) must be higher than a given value. For this reason, in Figures 11 and 17, and in practically all the separators, it can be observed an increasing trend before η reaches the zone of 80–100%. In this context, by only using the information in Figure 11 could have been enough for making a decision, which could thus have simplified this analysis. These considerations could make it possible to reformulate Equation (3). Thus, if the premises established in Section 3 can be accepted, and the flow developed is laminar with a clear dominance of the main phase over the friction in the pipe (Equation (15) is roughly fulfilled), it could be stated that:

$$\eta \approx \varphi \left(\frac{d}{2R}, \frac{L}{2R}, Re_a, \frac{Re_a}{C} \right), \tag{18}$$

which could allow future works to handle the design of these devices more easily. Regarding the analyses made in similar studies to this one [5,6,19–21], in the terms discussed in this section, it is worth mentioning that no dimensional analysis was carried out in them, so that it is difficult to make any further comparisons. Moreover, in [5,19–21] there was no discussion on the head losses h_{fk} (or the Euler number), the residence time t_r or the Froude number bound to each separator.

For its part, in [6] the variables h_{fk} and t_r have been determined for the separators tested there, which allows to summarily show their more representative values in Table 1. Likewise, in that table, other characteristic values of the separation tests done in [5,19–21] are given. For these studies, t_r and Re_a have been estimated, respectively, from Equations (7) and (9), taking into account the information reported in those works. Viewing the tabulated data, it is remarkable that there seems to be two different design proposals for helical separators: in references [5,19–21] wide helix radiuses (of 400 and 500 mm) are used, while in this study and in [6] narrow helix radiuses (of the order of 40 mm) are applied. In all the cases, t_r is less than 1–2 min, a much shorter time than that needed for a gravitational decanter (usually well above 12–24 h [4]).

Table 1. Characteristic values of the separation tests conducted in some works directly related to this study (C_{mp} refers to the concentration of the minority phase in each case).

Parameter	Ref. [6]	Refs. [5,20,21]	Ref. [19]	This Study
d (mm)	4.048	25.4	40	9.45
R (mm)	38.95	500	400	41.75
L (m)	10	31.4	15	4
q_t (cm^3/s)	<4.0	153	1456	<40
Re_a	<2000	7600	309	<60
Re_{crit}	7844	7400	7370	10500
h_{fk} (m.W.C)	1–3	–	–	<5.2
t_r (s)	30–80	105	24	<75
C_{mp} (%)	<2 (olive oil)	0.4 (mineral oil)	46.6 (water)	<13.3 (water)
η (%)	>95	<91	<80	80–100

In general, from the values shown, it could be inferred that narrow helix designs enable one to reach better yields, but the flow rates applied must be lower than in the wide radius cases. In water–oil systems [5,6,20,21], with olive oil or mineral oil as minority phases, the narrow helix design [6] allows the obtainment of better separation yields at oil concentrations of below 2%. In oil–water systems (this study and [19]), the narrow helix approach reaches better η values for water concentrations of up to 13.3%. Head losses h_{fk} and separation yields η are almost of the same order in [6] and in this study, but here the concentrations of the minority phase are higher. This fact makes it possible to consider the narrow helix design as being a valid approach to managing olive oil–water systems, which supports the idea that other alternatives (to the wide helix configuration) are possible in designing these devices.

4. Conclusions

Currently, one of the most important costs in industry is that related to energy consumption, so that the development of new equipment which could reduce this input is a field of research that still deserves to be addressed. In this work, the behavior of an alternative type of separator, orientated towards treating substances in two-phase flows, has been studied from a dimensional analysis viewpoint (an approach not applied in other studies directly related to this one). Specifically, four models of helical separators have been built and tested in order to handle olive oil and water two-phase flows. From the tests carried out with these devices, some results and questions are worth highlighting:

-　Due to the device's design and the characteristics of the hydraulic system used, the working flow rates have been below 140 l/h, which has resulted in Reynolds number values (Re_a) of below 60 in all cases. This circumstance has enabled all the tests to be performed under a laminar flow regime.
-　By analyzing the relationship between variables like the flow rate, the Reynolds number, the head losses and the water concentration present in the flows observed, it has been possible to establish a suitable operating area (not considered in other studies) that facilitates the existence of acceptable separation yields.
-　Specifically, it was observed that, for Re_a values > 15, it is feasible to obtain separation yields of the order of 80% to 100% in all the separators tested. Likewise, the energy required (head losses h_{fk}) in these cases has been in the range of 2 to 7 m.
-　Due to the experimental design applied, there was no direct relationship between the water concentration provided in each test with the flow rate processed. However, it was observed that the best separation yields η (of the order of 80% to 100%) are given, in general, for values of $C < 5\%$. A particularly significant case was the behavior of the separator with $R = 41.75$ mm and $L = 4$ m, which seems to maintain η above 80% even for $C > 5$–10%. However, and since the number of devices tested was small (only four) it is premature to assign a given relationship between the geometrical parameters used and the separation yields obtained.

- On making a careful study of the values of the ratio Re_a/C, it follows that it is possible to obtain adequate separations at moderate water concentrations ($C < 5\%$) if the level of energy available is high enough ($Re_a/C > 5$–10). For higher water concentrations ($C > 5\%$), it is inferred, from the data recorded, that adequate separations could be reached if the ratio $Re_a/C > 40$–70.
- The influence of some dimensionless terms, like the Euler number, tr^* or the Froude number, on the separation yield η can be considered (in this study) as being of second-order or computable through the Reynolds number Re_a. This fact means that, in cases like those presented in this work, these devices could be designed more easily.
- Considering the results obtained as a whole, it can be concluded that the separators built have served their purpose on a reduced scale, but more studies are understood to be required in order to improve their design and performance if it is desired to comply with the demands that any food industry could make on them. In particular, operating flow rates must be scaled to higher values while separation yield η and head losses h_{fk} should be reasonably maintained. This will probably affect the future selection of geometrical parameters such as $d, L,$ or R in a design context based on a narrow helix configuration (as an alternative to the wide helix designs proposed by other authors).

Author Contributions: P.V.-L. and M.R.-V. designed and ran the experiments. P.V.-L., M.R.-V. and I.P.-C. analyzed the data. P.V.-L. and I.P.-C. drafted and reviewed the manuscript. All authors have read and agreed to the published version of the manuscript.

Institutional Review Board Statement: Not applicable.

Informed Consent Statement: Not applicable.

Data Availability Statement: Not applicable.

Conflicts of Interest: The authors declare no conflict of interest.

Nomenclature

Symbols

A	Area of the pipe section	m^2
C	Water concentration	%
C_{mp}	Concentration of the minority phase	%
d	Pipe internal diameter	m
d_p	Inlet droplet diameter (of the dispersed fluid)	m
De	Dean number	–
De_a	Apparent Dean number	–
Eu	Euler number	–
Eu_a	Apparent Euler number	–
$f\,()$	Simple function (variable units)	/
f_a	Apparent friction factor, Equation (14)	–
f_{aI}	Apparent friction factor from Ito, Equation (15)	–
Fr	Froude number	–
g	Acceleration of gravity	m/s^2
h	Pressure head	m

h_{fk}	Headlosses, Equation (13)	m
H_i	Pressure head at the separator inlet	m
L	Separator length	m
q	Flow rate	m^3/s
q_{in}	Flow rate collected from the inner side of the separator	m^3/s
q_o	Olive oil flow rate	m^3/s
q_{out}	Flow rate collected from the outer side of the separator	m^3/s
q_t	Total flow rate	m^3/s
q_w	Water flow rate	m^3/s
q_{win}	Water flow rate from the inner side of the separator	m^3/s
q_{wout}	Water flow rate from the outer side of the separator	m^3/s
r	Pipe radius	m
R	Helix radius	m
Re	Reynolds number	–
Re_a	Apparent Reynolds number	–
R_{crit}	Critical Reynolds number	–
S_E	Standard error (variable units)	/
T	Fluid temperature	ºC
t_r	Residence time, Equation (7)	s
$t_r{}^*$	Dimensionless residence time, Equation (6)	–
u	Flow velocity	m/s
U	Average flow velocity	m/s
Uo	Olive oil average flow velocity (apparent value)	m/s
Z	Helix pitch	m
δ	Factor given by the ratio r/R	–
Δz	Difference in height between the separator ends (inlet and outlet)	m
γ	Surface tension	J/m^2
η	Separation yield	%
$\phi\ ()$	Multivariate function (variable units)	/
μ	Dynamic viscosity	Pa*s
μ_o	Olive oil dynamic viscosity	Pa*s
μ_w	Water dynamic viscosity	Pa*s
ν	Kinematic viscosity	m^2/s
ν_o	Olive oil kinematic viscosity	m^2/s
ρ	Fluid density	kg/m^3
ρ_o	Olive oil density	kg/m^3
ρ_ω	Water density	kg/m^3
$\Psi\ ()$	Multivariate function (variable units)	/

References

1. Uceda, M.; Jiménez, A.; Beltrán, G. Olive oil extraction and quality. Trends in olive oil production. *Grasas Aceites* **2006**, *57*, 25–31. [CrossRef]
2. Cerretani, L.; Gómez, A.M.; Bendini, A. Aspectos tecnológicos de la producción del aceite de oliva. In *El Aceite de Oliva Virgen: Tesoro de Andalucía*; Servicio de Publicaciones de la Fundación Unicaja: Málaga, Spain, 2010; Volume 6, pp. 171–193.
3. Altieri, G.; Di Renzo, G.C.; Genovese, F.; Tauriello, A.; D'Auria, M.; Racioppi, R.; Viggiani, L. Olive oil quality improvement using a natural sedimentation plant at industrial scale. *Biosyst. Eng.* **2014**, *122*, 99–114. [CrossRef]
4. Gila, A.; Sánchez-Ortiz, A.; Beltrán, G.; Bejaoui, A.; Aguilera, M.P.; Jiménez, A. Evolución durante el almacenamiento de las propiedades sensoriales de aceites de oliva vírgenes clarificados con diferentes sistemas. In *Proceedings of the Actas del XIX Simposio Científico-Técnico del Aceite de Oliva—Expoliva 2019, Jaén, Spain, 15–17 May 2019*; Fundación del Olivar: Mengíbar, Jaén, Spain, IND; Volume 43, pp. 1–8.
5. Zhao, L.; Xu, B.; Jiang, M.; Li, F.; Hua, Z. Flow–field distribution and parametric–optimisation analysis of spiral–tube separators. *Chem. Eng. Res. Des.* **2012**, *90*, 1011–1018. [CrossRef]
6. Vallesquino, P.; Molina, A. A study on the separation yield of helical tubes applied to water-olive oil two-phase flows. *Ing. Agua* **2019**, *23*, 169–185. [CrossRef]
7. Dean, W.R. Note on the motion of the fluid in a curved pipe. *Lond. Edinb. Dublin Philos. Mag. J. Sci.* **1927**, *4*, 208–223. [CrossRef]

8.   Hart, J.; Ellenberger, J.; Hamersma, P.J. Single-and two-phase flow through helically coiled tubes. *Chem. Eng. Sci.* **1988**, *43*, 775–783. [CrossRef]

9.   Kumar, V.; Nigam, K.D.P. Numerical simulation of steady flow fields in coiled flow inverter. *Int. J. Heat Mass Transf.* **2005**, *48*, 4811–4828. [CrossRef]

10.   Ciofalo, M.; Arini, A.; Di Liberto, M. On the influence of gravitational and centrifugal buoyancy on laminar flow and heat transfer in curved pipes and coils. *Int. J. Heat Mass Transf.* **2015**, *82*, 123–134. [CrossRef]

11.   Patankar, S.V.; Pratap, V.S.; Spalding, D.B. Prediction of turbulent flow in curved pipes. *J. Fluid Mech.* **1975**, *67*, 583–595. [CrossRef]

12.   Hüttl, T.J.; Friedrich, R. Influence of curvature and torsion on turbulent flow in helically coiled pipes. *Int. J. Heat Fluid Flow* **2000**, *21*, 345–353. [CrossRef]

13.   Di Liberto, M.; Di Piazza, I.; Ciofalo, M. Turbulence structure and budgets in curved pipes. *Comput. Fluids* **2013**, *88*, 452–472. [CrossRef]

14.   Bandaru, S.V.S.R.; Chhabra, R.P. Pressure drop for single and two-phase flow of non-newtonian liquids in helical coils. *Can. J. Chem. Eng.* **2002**, *80*, 315–321. [CrossRef]

15.   Vashisth, S.; Nigam, K.D.P. Prediction of flow profiles and interfacial phenomena for two-phase flow in coiled tubes. *Chem. Eng. Process. Process Intensif.* **2009**, *48*, 452–463. [CrossRef]

16.   Saffari, H.; Moosavi, R.; Nouri, N.M.; Lin, C.X. Prediction of hydrodynamic entrance length for single and two-phase flow in helical coils. *Chem. Eng. Process. Process Intensif.* **2014**, *86*, 9–21. [CrossRef]

17.   Gourma, M.; Verdin, P.G. Two-phase slug flows in helical pipes: Slug frequency alterations and helicity fluctuations. *Int. J. Multiph. Flow* **2016**, *86*, 10–20. [CrossRef]

18.   Vidnes, J.; Engvik, S.A. Analysis of Compact Separation Systems and Experimental Study of Centrifugal Separation in Helically Coiled Pipes. Master's Thesis, Department of Production and Quality Engineering, Norwegian University of Science and Technology,, Trondheim, Norway, 2015.

19.   Zhang, J.; Guo, J.; Gong, D.T.; Wang, L.Y.; Tang, C.; Zheng, Z.C. An investigation on oil/water separation mechanism inside helical pipes. *J. Hydrodyn.* **2006**, *18*, 336–340. [CrossRef]

20.   Zhao, L.; Xu, L.; Hua, Z.; Ma, Z.; Cao, H. Numerical simulation and experimental study on helical pipe oil–water separator for deoiling. In Proceedings of the 3rd International Conference on Bioinformatics and Biomedical Engineering, IEEE, Beijing, China, 11–13 June 2009; pp. 1–4. [CrossRef]

21.   Niu, D.; Zhao, L.; Hua, Z. Performance study of de-oiling spiral tube separators. In Proceedings of the 4th International Conference on Bioinformatics and Biomedical Engineering, IEEE, Chengdu, China, 18–20 June 2010; pp. 1–4. [CrossRef]

22.   Singh, R.P.; Heldman, D.R. *Introduction to Food Engineering*; Elsevier–Academic Press: London, UK, 2009.

23.   Sánchez, M.; Vallesquino, P. Estudio de la Densidad y la Viscosidad en Emulsiones de Aceite de Oliva y Agua. Bachelor Thesis, Facultad de Veterinaria, Universidad de Córdoba, Córdoba, Spain, 2018.

24.   Hermida, J.R. *Fundamentos de Ingeniería de Procesos Agroalimentarios*; Mundi-Prensa: Madrid, Spain, 2000.

25.   Levenspiel, O. *Flujo de Fluidos e Intercambio de Calor*; Reverté: Barcelona, Spain, 1996.

26.   Trallero, J.L.; Sarica, C.; Brill, J.P. A study of oil/water flow patterns in horizontal pipes. *SPE Prod. Facil.* **1997**, 165–172. [CrossRef]

27.   Srinivasan, P.S.; Nandapurkar, S.S.; Holland, F.A. Friction factors for coils. *Trans. Inst. Chem. Eng.* **1970**, *48*, T156–T161.

28.   Mafart, P.; Béliard, E. *Ingeniería Industrial Alimentaria*; Acribia: Zaragoza, Spain, 1994; Volume II.